Ann. Inst. H. Poincaré D
Comb. Phys. Interact. 12 (2025), 787–818
DOI 10.4171/AIHPD/202

Lineup polytopes of products of simplices

Federico Castillo and Jean-Philippe Labbé

Abstract. Consider a real point configuration A of size n and an integer $r \leq n$. The vertices of the r-lineup polytope of A correspond to the possible orderings of the top r points of the configuration obtained by maximizing a linear functional. The motivation behind the study of lineup polytopes comes from the representability problem in quantum chemistry. In that context, the relevant point configurations are the vertices of hypersimplices and the integer points contained in an inflated regular simplex. The central problem consists in providing an inequality representation of lineup polytopes as efficiently as possible. In this article, we adapt the developed techniques to the quantum information theory setup. The appropriate point configurations become the vertices of products of simplices. A particular case is that of lineup polytopes of cubes, which form a type B analog of hypersimplices, where the symmetric group of type A naturally acts. To obtain the inequalities, we center our attention on the combinatorics and the symmetry of products of simplices to obtain an algorithmic solution. Along the way, we establish relationships between lineup polytopes of products of simplices with the Gale order, standard Young tableaux, and the resonance arrangement.

1. Introduction

The Farkas–Minkowski–Weyl theorem establishes a duality principle which is fundamental in discrete geometry: convex polyhedra admit two different equivalent representations [34, Theorem 7.1]. Either they represent the set of solutions of a system of linear inequalities (H-representation) or they are sums of a linear subspace, a pointed cone, and a polytope (V-representation). Certain problems—for example, asking whether a point belongs to a convex polyhedron, the so-called *membership problem*—are easily solvable if one has access to its H-representation, but not if one only has its V-representation. The reverse direction is similarly true, making the translation between representations a task of major importance which is well known to be computationally expensive [3]. This problem is sometimes referred to as the *representation conversion problem* or the *convex hull problem*. The existence of a polynomial

Mathematics Subject Classification 2020: 52B55 (primary); 52B12, 90C06, 81P99 (secondary).
Keywords: convex hull problem, symmetric polytopes, quantum marginal problem, normal fans, recursive algorithm.

time translation algorithm appears to be unlikely as it is NP-complete for unbounded polyhedra [19]. It remains an open problem to determine whether there is a translation algorithm that runs polynomially (on the size of input and output) for bounded polyhedra [17, Open Problem 26.3.4]. By exploiting symmetry of polyhedra, it is possible to obtain more efficient algorithms using the related geometric and combinatorial objects, such as fundamental domains and posets. Indeed, in the present paper, we adapt a $(V \to H)$-translation algorithm introduced in [11] and extend its use to another family of symmetric polytopes: lineup polytopes of product of simplices. Aside from their geometric origin, it turns out that lineup polytopes of product of simplices show relations to quantum information theory [22], to the White Whale [15], and to applications of standard Young tableaux in deconvolution in mathematical statistics [24, 25].

Quantum marginal problem. The motivation for extending this algorithm to the product of simplices comes from quantum information theory. Almost 20 years ago, Klyachko used tools from representation theory to study the quantum marginal problem (QMP), details of which are provided in his unpublished manuscript [21]. His main contribution is an H-representation of the (moment) polytope of all compatible marginals. Each inequality in the representation has physical significance: it gives a linear constraint on the allowable marginals that are simple to test in practice. The more general problem of providing an H-representation of moment polytopes has been treated by Berenstein–Sjaamar [6], Ressayre [30], and Vergne–Walter [38]. All of these H-representations are hard to make effective in practice. In the article [11], we lay out discrete geometric and combinatorial methods in order to circumvent the complexity of Klyachko's framework by relaxing the problem and computing a larger polytope *while keeping the physically relevant portion* of Klyachko's solution. The main geometric tool introduced therein is *lineup polytopes*, whose H-representations provide necessary linear inequalities that we can effectively compute.

Parallel computational tools and symmetry. There are several translating algorithms between the V- and H-representations that are already implemented; see [4, 12, 14, 31] for some examples. Each algorithm seems to do well on certain classes of polytopes, but none always stands out. In the present study, we examine a particular family and tailor our methods to that context. We start with a known normal fan and the goal is to compute a specific refinement of it. We define lineup fans to serve as intermediate steps, obtained by successive refinements. The refinement is obtained by adding certain hyperplanes to each full-dimensional cone of the intermediate fans. This idea is similar to the one behind the *incremental* algorithms which compute convex hulls by adding one hyperplane at a time. The refinement of a fan naturally lends itself to parallelization; for a recent study on parallelization of general $(V \to H)$-algorithms, see [5]. Another feature allowing us to speed the computations is the presence of symmetry. The family of polytopes at play is highly symmetric and we exploit this fact to compute orbit representatives instead of all of them. Finally, the combinatorics of the problem at hand provide a poset leading to the refinements needed at each step. The resulting algorithms provide output-polynomial time procedures to provide (symmetrically reduced) V- and H-representations of lineup polytopes of products of simplices.

White Whale. Lineup polytopes of hypercubes (i.e., products of line segments) are related to the *resonance arrangement*; see Remark 4.6. This arrangement has the universal property that any rational hyperplane arrangement is the minor of some large enough resonance arrangement [23]. The corresponding zonotope, known as the White Whale, is the Minkowski sum of all 0/1 vectors of length N. There has been interest in computing the number of vertices, but even with the latest available method, the problem remains elusive for $N > 9$ [15].

Realizable tableaux. Another case appeared in disguise in earlier work. The lineup polytope of the product of two simplices $\Delta_{e-1} \times \Delta_{f-1}$ of dimension $(e + f - 2)$ is related to the number of *realizable* standard Young tableaux (SYT) of rectangular shape $e \times f$, as observed by Klyachko in [21]. Realizable SYT are also called *outer sums* and they are systematically studied by Mallows and Vanderbei [25]. They appear also in the recent work of Black and Sanyal [7]. Contrary to the set of all SYT, which has a closed product formula (the hook length formula [18]), there is no enumeration formula for the realizable case. Recently, Araujo, Black, Burcroff, Gao, Krueger, and McDonough provide some asymptotic results for realizable SYT of rectangular shape in [2]. Therein, they prove that, with e fixed, the number of such tableaux is exponential in f, but the base of the exponential is still unknown. Our computations shed a light on what that base may be; see Section 3.2.1.

Organization of the paper. In Section 2, we provide the preliminaries on polytopes, their normal fans, lineup polytopes, the connection to the physical motivation and describe important examples. In Section 3, we develop general results for lineups of product of simplices along with the algorithmic method. In Section 4, we specialize our tools to the particular case of products of line segments. In Section 5, we finish with some observations about the original quantum marginal problem and lineup polytopes of cyclic polytopes.

2. Preliminaries

We adopt the following conventions: $d \in \mathbb{N} \setminus \{0\}$, $[d] := \{1, 2, \ldots, d\}$. The cardinality of a set S is denoted by $|S|$. Let $\mathbb{R}^d$ be the d-dimensional Euclidean space with elementary basis $\{\boldsymbol{e}_i : i \in [d]\}$ and inner product given by $\langle \boldsymbol{e}_i, \boldsymbol{e}_j \rangle = \delta_{i,j}$ for $i, j \in [d]$. Whenever a vector $\mathbf{v} \in \mathbb{R}^d$ is written as a tuple $(v_1, \dots, v_d)$, the entries are expressing the coefficients of $\mathbf{v}$ in the standard basis, i.e., $\mathbf{v} = \sum v_i \mathbf{e}_i$.

2.1. Polytopes and normal fans

A *polyhedron* is the intersection of finitely many closed half-spaces [34, Chapter 7]:

$$\mathsf{Q} := \{\mathbf{x} \in \mathbb{R}^d : M\mathbf{x} \leq \mathbf{b}\}, \tag{2.1}$$

where M is a matrix and $\mathbf{b}$ is a vector. The expression in (2.1) is a *H-representation* of Q. A row of M and its corresponding entry in $\mathbf{b}$ give a *defining inequality* of Q and represent a closed half-space containing Q. If a row of M and its corresponding entry in $\mathbf{b}$ are a positive linear combination of other rows of M and their corresponding entries in $\mathbf{b}$, it is not necessary to define Q, and this H-representation is called *redundant*.

Let $\mathbf{A} = \{\mathbf{v}_1, \dots, \mathbf{v}_n\} \subset \mathbb{R}^d$. We refer to $\mathbf{A}$ as a *point configuration of size n*. The *affine hull* aff($\mathbf{A}$) of $\mathbf{A}$ is the set of vectors $\sum_{i=1}^n \lambda_i \mathbf{v}_i$ such that $\sum_{i=1}^n \lambda_i = 1$ and $\lambda_i \in \mathbb{R}^d$. The *conical* (or "positive") *hull* cone($\mathbf{A}$) of $\mathbf{A}$ is the set of vectors $\sum_{i=1}^n \lambda_i \mathbf{v}_i$ such that $\lambda_i \geq 0$, defining a *cone*. A cone is *pointed* if it contains no lines. The *convex hull* conv($\mathbf{A}$) of $\mathbf{A}$ is the set of vectors $\sum_{i=1}^n \lambda_i \mathbf{v}_i$ such that $\sum_{i=1}^n \lambda_i = 1$ and $\lambda_i \geq 0$, defining a *polytope*. The elements in these sets are called *affine*, *conical*, and *convex combinations* of $\mathbf{A}$, respectively. We refer to the elements of minimal generating sets (in $\mathbf{A}$) of affine, conical, and convex hulls as *line generators*, *ray generators*, and *vertices*. Line generators are unique up to change of affine basis and ray generators are unique up to scaling by positive scalars.

By the Farkas–Minkowski–Weyl theorem, every polyhedron Q can be decomposed uniquely as the sum of an affine hull, a conical hull, and a convex hull:

$$\mathsf{Q} = \mathsf{L} + \mathsf{K} + \mathsf{P}, \tag{2.2}$$

where L is a linear subspace (called the *lineality space* of Q), K is a pointed cone (called the *recession cone* of Q), and P is a polytope. The expression in (2.2) is the *V-representation* of Q. Thus, polytopes and cones are polyhedra: polytopes are *bounded* polyhedra and cones are *homogeneous* polyhedra, that is, $\mathbf{b} = \mathbf{0}$ in (2.1).

Remark 2.1. Translating between V- and H-representations of affine or linear subspaces is done quite efficiently through Gauss elimination. For polytopes or pointed cones, this process is known to be much harder and a central subject in linear optimization and discrete geometry as mentioned in the introduction.

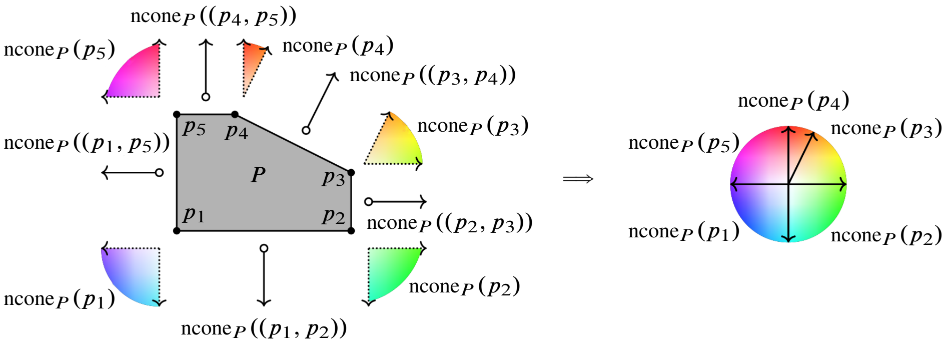

Figure 1. A 2-dimensional polytope and its normal fan obtained by placing the normal cones of the vertices of P at the origin.

2.1.1. Adopted technique: Exploiting duality. We restrict ourselves to the case of polytopes with a high level of symmetry. In order to pass from a V- to a H-representation, we use the following method. Effectively, it turns a $(V \to H)$-translation into a $(H \to V)$-translation which is easier to handle in the special cases of interest.

Let $\mathsf{P} = \mathrm{conv}(\mathbf{A})$ be a polytope. A linear inequality satisfied by all points $\mathbf{x} \in \mathsf{P}$ is called *valid*. The *support function* $h_{\mathsf{P}} : \mathbb{R}^d \to \mathbb{R}$ of P is defined as $h_{\mathsf{P}}(\mathbf{y}) := \max_{\mathbf{x}\in\mathsf{P}}\langle \mathbf{y}, \mathbf{x}\rangle$. Every vector $\mathbf{y} \in \mathbb{R}^d$ induces a unique valid inequality on a polytope P, according to $\langle \mathbf{y}, \mathbf{x}\rangle \leq h_{\mathsf{P}}(\mathbf{y})$. The polytope $\mathsf{P}^{\mathbf{y}} = \{\mathbf{x} \in \mathsf{P} : \langle \mathbf{y}, \mathbf{x}\rangle = h_{\mathsf{P}}(\mathbf{y})\}$ is refered to as a *face* of P. Vertices of P are 0-dimensional faces and *facets* of P are codimension-1 faces. Given a face F of P, we define its *open* and *closed normal cones*:

$$\begin{aligned} \mathrm{ncone}_{\mathsf{P}}(\mathsf{F})^{\circ} &:= \{\mathbf{y} \in \mathbb{R}^d : \mathsf{P}^{\mathbf{y}} = \mathsf{F}\}, \\ \mathrm{ncone}_{\mathsf{P}}(\mathsf{F}) &:= \{\mathbf{y} \in \mathbb{R}^d : \mathsf{P}^{\mathbf{y}} \supseteq \mathsf{F}\}. \end{aligned} \tag{2.3}$$

The collection $\mathcal{N}(\mathsf{P}) := \{\mathrm{ncone}_{\mathsf{P}}(\mathsf{F}) : \mathsf{F} \text{ a face of } \mathsf{P}\}$ is the *normal fan* of P. Here is the keystone of the approach: the normal fan of a polytope is *entirely recovered* from the normal cones of the vertices, since their faces *are* all the other cones in the fan as the following example illustrates.

Example 2.2 (Normal fan of a polygon on the plane). Let

$$\mathsf{P} = \mathrm{conv}\{(0,0), (3,0), (3,1), (1,2), (0,2)\}$$

in $\mathbb{R}^2$, as illustrated in Figure 1.

To go from a V- to an H-representation, one first determines the normal cones of the vertices, then obtain all rays, and finally get a non-redundant H-representation:

(i) The definitions in equations (2.3) say that the normal cone of a face F consists of all vectors $\mathbf{y}$ whose linear functional is maximized on F. Whence, for each vertex $\mathbf{v}$ of P, its normal cone has the following H-representation:

$$\mathrm{ncone}_{\mathsf{P}}(\mathbf{v}) = \{\mathbf{y} \in \mathbb{R}^d : \langle \mathbf{y}, \mathbf{v} - \mathbf{v}' \rangle \geq 0, \text{ for } \mathbf{v}' \in \mathbf{A}\}. \tag{2.4}$$

(ii) Decompose the normal cone into its lineality space and its recession cone as in (2.2), i.e., $\mathrm{ncone}_{\mathsf{P}}(\mathbf{v}) = \mathsf{L}_{\mathsf{P}}(\mathbf{v}) + \mathsf{K}_{\mathsf{P}}(\mathbf{v})$. (There is no polytope factor in this case.) The lineality space $\mathsf{L}_{\mathsf{P}}(\mathbf{v})$ is the orthogonal complement of $\mathrm{aff}(\mathsf{P})$; hence, it does not depend on $\mathbf{v}$.

(iii) Translate the H-representation of $\mathsf{K}_{\mathsf{P}}(\mathbf{v})$ to a V-representation:

$$\mathsf{K}_{\mathsf{P}}(\mathbf{v}) = \left\{ \sum_{i=1}^{j} \lambda_i \mathbf{r}_i : \lambda_i \geq 0, \text{ for } i \in [j] \right\}$$

for some $\mathbf{r}_1, \ldots, \mathbf{r}_j \in \mathbb{R}^d$.

(iv) Let $\mathbf{B}$ be the set of all ray generators $\mathbf{r}_i$'s found in the previous step for all $\mathrm{ncone}_{\mathsf{P}}(\mathbf{v})$. For each $\mathbf{r} \in \mathbf{B}$, we determine the value of $h_{\mathsf{P}}(\mathbf{r})$ by evaluating it on $\mathbf{A}$.

Let $\mathbf{C}$ be a basis of L_{P}. We end up with the non-redundant H-representation

$$\mathsf{P} = \big\{ \mathbf{x} \in \mathbb{R}^d : \langle \mathbf{r}, \mathbf{x} \rangle \leq h_{\mathsf{P}}(\mathbf{r}) \text{ for all } \mathbf{r} \in \mathbf{B} \\ \langle \mathbf{y}, \mathbf{x} \rangle = h_{\mathsf{P}}(\mathbf{y}) \text{ for all } \mathbf{y} \in \mathbf{C} \big\}.$$

In what follows, we will see that the high level of symmetry of the studied polytopes confers optimal efficiency to this approach. Indeed, the exponential number of vertices to consider is reduced to a minimum. Furthermore, the description in equation (2.4) is reduced to treating only one linear functional and vertex per orbit. The main remaining piece is the ($H \to V$)-translation in the third step.

2.2. Lineup polytopes

Let $\mathbf{A} = \{\mathbf{v}_1, \ldots, \mathbf{v}_n\} \subset \mathbb{R}^d$ and $\boldsymbol{y} \in \mathbb{R}^d$. A generic vector $\boldsymbol{y}$ provides an injective linear functional $\langle \boldsymbol{y}, \cdot \rangle : \mathbb{R}^d \to \mathbb{R}$ that totally orders the elements of $\mathbf{A}$ from maximal to minimal value. Given such a total order and an integer r such that $1 \leq r \leq n$, the sequence ℓ of the first r elements in this total order is called a *lineup of length* r of $\mathbf{A}$ [11, Definition 6.1]. Let $\boldsymbol{w} := (w_1, w_2, \ldots, w_r)$ be such that $1 > w_1 > w_2 > \cdots > w_r > 0$ and $\sum_{i=1}^r w_i = 1$, and furthermore, let $\ell = (\boldsymbol{v}_1, \boldsymbol{v}_2, \ldots, \boldsymbol{v}_r)$ be an ordered list of r vectors of $\mathbf{A}$. We refer to the w_i's as *weights*. The *occupation vector* associated to ℓ with respect to $\boldsymbol{w}$ is $\mathbf{o}_{\boldsymbol{w}}(\ell) := \sum_{i=1}^r w_i \boldsymbol{v}_i$. The r-*lineup polytope* of $\mathbf{A}$ is

$$\mathsf{L}_{r,\boldsymbol{w}}(\mathbf{A}) := \mathrm{conv}\{\mathbf{o}_{\boldsymbol{w}}(\ell) : \ell \text{ is an ordered } r\text{-subset of } \mathbf{A}\};$$

see [11, Definition 6.1]. To a polytope $\mathsf{P} \subset \mathbb{R}^d$ we associate the point configuration $\mathbf{A}$ given by listing its vertices in some order. The next proposition summarizes the content of [11, Theorem E]; part (3) is a slight generalization of [11, Proposition 6.18].

Proposition 2.3. *Let $\mathbf{A} = \{\mathbf{v}_1, \dots, \mathbf{v}_n\} \subset \mathbb{R}^d$ and $1 \le r \le n$. If $\boldsymbol{w} \in \mathbb{R}^r$ has strictly decreasing coordinates, then the following statements hold.*

(1) *The point $\mathbf{o}_{\boldsymbol{w}}(\ell)$ is a vertex of the lineup polytope $\mathsf{L}_{r,\boldsymbol{w}}(\mathbf{A})$ if and only if ℓ is an r-lineup.*

(2) *If $\boldsymbol{v}^\ell$ is a vertex of $\mathsf{L}_{r,\boldsymbol{w}}$ with lineup $\ell = (\boldsymbol{v}_1, \dots, \boldsymbol{v}_r)$, then the open normal cone of $\boldsymbol{v}^\ell$ is the set of $\boldsymbol{y} \in \mathbb{R}^d$ such that*

$$\begin{aligned} &\langle \boldsymbol{y}, \boldsymbol{v}_1\rangle > \langle \boldsymbol{y}, \boldsymbol{v}_2\rangle > \cdots > \langle \boldsymbol{y}, \boldsymbol{v}_r\rangle \\ \text{and}\quad &\langle \boldsymbol{y}, \boldsymbol{v}_r\rangle > \langle \boldsymbol{y}, \boldsymbol{v}\rangle \quad \textit{for every point } \boldsymbol{v} \textit{ of } \mathbf{A} \textit{ not contained in } \ell. \end{aligned}$$

The normal cone of $\boldsymbol{v}^\ell$ is called the lineup cone of ℓ.

(3) *If $\boldsymbol{s}(\boldsymbol{y}, \mathbf{A})$ denotes the largest r values of $\langle \boldsymbol{y}, \mathbf{A}\rangle$ ordered decreasingly, then*

$$\max_{\boldsymbol{x} \in \mathsf{L}_{r,\boldsymbol{w}}(\mathbf{A})} \langle \boldsymbol{y}, \boldsymbol{x}\rangle = \langle \boldsymbol{w}, \boldsymbol{s}(\boldsymbol{y}, \mathbf{A})\rangle.$$

Lineup cones are independent of the specific values of the entries of $\boldsymbol{w}$ as long as they are strictly decreasing. Therefore, the normal fan $\Sigma^r(\mathbf{A})$ is independent of the specific choice of $\boldsymbol{w}$ and we call it the *lineup fan* of $\mathbf{A}$. For this reason, we omit the symbol $\boldsymbol{w}$ in our notation. Also, when $r = n$, we omit the symbol r and call $\mathsf{L}_{n,\boldsymbol{w}}(\mathbf{A}) = \mathsf{L}(\mathbf{A})$ the *sweep polytope* of $\mathbf{A}$. These polytopes were studied by Padrol and Philippe; see [27]. Sweep polytopes are zonotopes:

$$\mathsf{L}(\mathbf{A}) = \sum_{\boldsymbol{v}_1, \boldsymbol{v}_2 \in \mathbf{A}} \operatorname{conv}(\boldsymbol{v}_1, \boldsymbol{v}_2).$$

Finding the H-representation of an arbitrary Minkowski sum is computationally hard [37]. Even for the case of zonotopes, it is still an open problem find an efficient algorithm; see [16, Lecture 4]. An example of a particular zonotope whose H-computation has received recent attention is treated in more detail below in Remark 4.6.

However, the general definition with $r < |\mathbf{A}| = n$ allows us to partially compute the normal fan of the sweep polytope using recursion. Indeed, we have

$$\mathcal{N}(\operatorname{conv}(\mathbf{A})) = \Sigma^1(\mathbf{A}) \succeq \Sigma^2(\mathbf{A}) \succeq \cdots \succeq \Sigma^n(\mathbf{A}) = \mathcal{N}(\mathsf{L}(\mathbf{A})), \tag{2.5}$$

where $\Sigma \succeq \Sigma'$ denotes that Σ' is a refinement of Σ.

Remark 2.4. Equation (2.5) delivers partial information on the whole sweep polytope without fully computing it. This feature is interesting on its own right as it is possible to obtain relevant information (a non-redundant and partial facet-defining H-representation) for a potentially large polytope without having to wait for the translation algorithm to complete.

2.3. Connections with physics

We describe the physical context related to the study of lineup polytopes of products of simplices. We start with the simplest instance of the Quantum Marginal Problem (for a general account of it see [33]). Let $\mathcal{H}_1$, $\mathcal{H}_2$ be two finite-dimensional Hilbert spaces. There is a linear map called the *partial trace* between $\operatorname{End}(\mathcal{H}_1 \otimes \mathcal{H}_2)$ and $\operatorname{End}(\mathcal{H}_1)$ uniquely determined by mapping

$$\rho_1 \otimes \rho_2 \mapsto \operatorname{trace}(\rho_2)\rho_1$$

whenever ρ_1, ρ_2 are linear operators on $\mathcal{H}_1$ and $\mathcal{H}_2$, respectively. Using the partial trace, we associate to an operator $\rho \in \operatorname{End}(\mathcal{H}_1 \otimes \mathcal{H}_2)$ its *marginals* $\rho^{(1)}$ and $\rho^{(2)}$, which are the partial traces of ρ with respect to $\mathcal{H}_1$ and $\mathcal{H}_2$, respectively. Furthermore, if we assume that ρ is a density operator (that is, if all its eigenvalues are real, in the interval [0, 1], and they add up to 1), then its two marginals $\rho^{(i)}$ are density operators too. In this context, the quantum marginal problem is to determine the triples $(\boldsymbol{w}, \boldsymbol{w}^{(1)}, \boldsymbol{w}^{(2)})$ such that there exists an operator ρ such that

$$\boldsymbol{w} = \operatorname{spec}(\rho) \quad \text{and} \quad \boldsymbol{w}^{(i)} = \operatorname{spec}(\rho^{(i)}) \quad \text{for } i = 1, 2.$$

The setup naturally generalizes to the tensor product of $N \geq 2$ Hilbert spaces each of dimension d: we seek to relate the spectrum of a density operator on the tensor space with the spectra of its N marginals. This space parametrizes the states of a system of N distinguishable particles, called qu$d$its, if we want to refer to the dimension d. We will give special attention to the case $d = 2$ because it corresponds to systems of qubits relevant in quantum information. This instance of the Quantum Marginal Problem was solved by Klyachko and Altunbulak; see [1,22]. For any vector $\boldsymbol{x} \in \mathbb{R}^d$, we define $\boldsymbol{x}^{\downarrow}$ as the vector consisting of the absolute values of the entries of $\boldsymbol{x}$ in weakly decreasing order. The set

$$\Lambda(d, N, \boldsymbol{w}) := \Big\{(\boldsymbol{v}^1, \dots, \boldsymbol{v}^N) \in \prod_{i=1}^{N} \mathbb{R}^d \mid \exists\, \rho \text{ with } \operatorname{spec}(\rho) = \boldsymbol{w} \text{ and } \operatorname{spec}(\rho^{(i)})^{\downarrow} = \boldsymbol{v}^i, \text{ for all } i \in [N]\Big\} \tag{2.6}$$

of spectra of the marginals arising from operators with a fixed spectrum $\boldsymbol{w}^{\downarrow}$ is a polytope. Polytopality is a consequence of general results about moment polytopes [20].

Klyachko described a finite set of defining inequalities in [22, Theorem 4.2.1] and [1, Example 2]. His solution has two steps:

(1) (Discrete geometry) Find all *edges* of certain polyhedral cones called *cubicles*.

(2) (Schubert calculus) For each *edge*, consider all permutations satisfying certain cohomological conditions that can be phrased in terms of Schubert polynomials.

Each pair (edge, permutation) produces a defining inequality for the polytope $\Lambda(d, N, \boldsymbol{w})$ [1, (13)]. Both steps are theoretical triumphs; however, in practice, they retain a high computational complexity. Our motivation for the present paper is to efficiently compute the first part of the solution.

The polytope $\Lambda(d, N, \boldsymbol{w})$ is not a lineup polytope; however, it is closely related to $\mathsf{L}(\Pi_{d,N})$, the lineup polytope of the product of N simplices of dimension $d - 1$. There is a region which we call the *test cone* (equation (3.1)) for which the support functions of both polytopes agree. This means that we can get some of the defining inequalities of $\Lambda(d, N, \boldsymbol{w})$ by means of computing $\mathsf{L}(\Pi_{d,N})$. The polytope $\Lambda(d, N, \boldsymbol{w})$ is always contained in $\mathsf{L}(\Pi_{d,N})$, and as an approximation, one can consider $\mathsf{L}(\Pi_{d,N})$ intersected with the test cone. See the flower diagram of [11, Figure 6].

2.4. Examples

Example 2.5 ($[n, m]$-grid). Let $\mathbf{A} = \{1, 2, \ldots, n\} \times \{1, 2, \ldots, m\} \subset \mathbb{R}^2$ and set $r = mn$. The number of r-lineups, or sweeps, is equal to the number of vertices of the sweep polytope of $\mathbf{A}$. Since this is a polygon, the number of vertices is equal to the number of edges and this corresponds to uncoarsenable rankings. In this context, a ranking is uncoarsenable as long as the corresponding functional puts two points in a tie. By symmetry, we can assume without loss of generality that $(1, 1)$ comes first in the ranking. So, we must count the number of line segments with one endpoint in $\{(1, 1), \ldots, (n, 1)\}$, the other in $\{(1, 1), \ldots, (1, m)\}$, up to parallel translations. By counting the slopes in lowest fractional terms, we find that the number of parallel classes is

$$\sum_{i=1}^{n} \phi(i, m) + 2 = \sum_{i=1}^{m} \phi(i, n) + 2,$$

where

$$\phi(a, b) = |\{k \in [b] : \gcd(k, a) = 1\}|.$$

The $+2$ comes from the segments parallel to the axes. Considering symmetry, we have

$$4\left(\sum_{i=1}^{n} \phi(i, m)\right) + 2$$

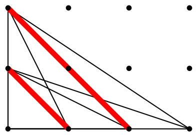

Figure 2. Eight line segments between the points in both axes, but two of them are parallel, so they correspond to the same ranking.

uncoarsenable rankings, and thus also the same number of sweeps. If we assume that $n > m$, we can bound

$$\sum_{i=1}^{n} \phi(i,m) = \sum_{i=1}^{m} \phi(i,m) + \sum_{i=m+1}^{n} \phi(i,m) < m^2 + \sum_{i=1}^{n} \varphi(i),$$

where $\varphi(i) = \phi(i,i)$ is Euler's totient function. For the latter sum, we have that

$$\sum_{i=1}^{n} \varphi(i) = \frac{1}{2}\left(1 + \sum_{i=1}^{n} \mu(i) \left\lfloor \frac{n}{i} \right\rfloor^2\right) = \frac{3}{\pi^2} n^2 + O\big(n (\log n)^{\frac{2}{3}} (\log\log n)^{\frac{4}{3}}\big),$$

see [39], which leads to a bound of $4m^2 + 12n^2/\pi^2$ for the number of uncoarsenable rankings, which is much smaller than $(nm)!$. For example, when $(m,n) = (4,3)$, the sweep polytope is the convex hull of $12! = 479\,001\,600$ points. However, we obtain only 38 sweeps so that the resulting sweep polygon has 38 vertices, and thus 38 edges, see Figure 2.

Example 2.6. Let P be the prism over the two-dimensional triangle

$$\mathsf{T} = \operatorname{conv}\{(0,0,0), (0,1,0), (0,0,1)\}$$

and $\boldsymbol{w} = (6,5,4,3,2,1)/21$. The lineup polytope $\mathsf{L}_{6,\boldsymbol{w}}(\mathsf{P})$ of P is depicted in Figure 3. The size of this example is quite small and the naive approach is efficient enough to provide its description in SageMath. Its f-vector is $(60, 90, 32)$; it has 12 square facets, 14 hexagonal facets, and 6 octagonal facets. There is a correspondence between facets and cocircuits of the point configurations; see, e.g., [27, Section 1.1] for further details on this correspondence.

Example 2.7 (Standard simplex). Let $\mathbf{A} = \{\boldsymbol{e}_1, \dots, \boldsymbol{e}_d\}$ be the canonical basis of $\mathbb{R}^d$. The convex hull $\operatorname{conv}(A)$ is the *standard simplex* of dimension $(d-1)$ and it is denoted by Δ_{d-1}. The sweep polytope $\mathsf{L}_{d,\boldsymbol{w}}(\mathbf{A})$ in this case is equal to

$$\operatorname{conv}\{w_{\pi(1)}, w_{\pi(2)}, \dots, w_{\pi(d)} \mid \pi \in \mathfrak{S}_d\},$$

known as a *permutohedron*; see [29].

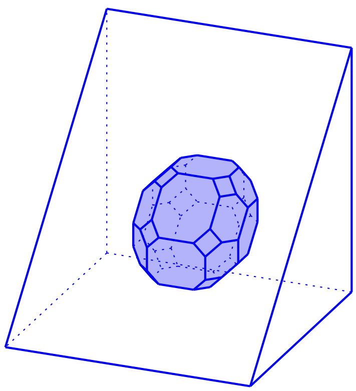

Figure 3. The lineup polytope of the prism over a triangle with weights $(6, 5, 4, 3, 2, 1)/21$.

Example 2.8 (Product of two segments, or the $[-1, 1]$-square). The polytope $\Delta_1 \times \Delta_1$ is a square in $\mathbb{R}^2 \times \mathbb{R}^2 = \mathbb{R}^4$ with vertices

$$\{(1, 0; 1, 0), (1, 0; 0, 1), (0, 1; 1, 0), (0, 1; 0, 1)\}.$$

To lower the dimension of the ambient space, we map

$$\gamma : \mathbb{R}^2 \times \mathbb{R}^2 \to \mathbb{R}^2, \quad (x_{11}, x_{12}; x_{21}, x_{22}) \mapsto (x_{11} - x_{12}, x_{21} - x_{22}).$$

Under this projection, the polytope $\Delta_1 \times \Delta_1$ maps to the square $[-1, 1] \times [-1, 1]$ in $\mathbb{R}^2$. The 24 occupation vectors are illustrated in Figure 4 along with their convex hull. In the figure, the points 14 and 23 are not necessarily in that order along the x-axis. The order depends on the choice of vector $\mathbf{w}$. To obtain Figure 4, one could take $\frac{1}{10}(7, 2, 1, 0)$. See Example 5.1 for more details.

The convex hull is the polyhedron consisting of all points $(x_1, x_2) \in \mathbb{R}^2$ satisfying the following linear inequalities:

$$\begin{aligned} -w_1 - w_2 + w_3 + w_4 \le x_1 \qquad &\le w_1 + w_2 - w_3 - w_4, \\ -w_1 - w_2 + w_3 + w_4 \le \qquad x_2 &\le w_1 + w_2 - w_3 - w_4, \\ -2w_1 + 2w_4 \le x_1 + x_2 &\le 2w_1 - 2w_4, \\ -2w_1 + 2w_4 \le x_1 - x_2 &\le 2w_1 - 2w_4. \end{aligned} \tag{2.7}$$

Recall from Section 2.3 that, for any vector $\boldsymbol{x} \in \mathbb{R}^d$, we define $\boldsymbol{x}^{\downarrow}$ as the vector consisting of the absolute values of the entries of $\boldsymbol{x}$ in weakly decreasing order. Using that notation, the H-representation of the sweep polytope $\mathsf{L}(\square_2)$ of the square $\square_2 = [-1, 1] \times [-1, 1]$ given in equation (2.7) can be rewritten as

$$\mathsf{L}(\square_2) = \left\{ \boldsymbol{x} \in \mathbb{R}^2 : \begin{pmatrix} 1 & 0 \\ 1 & 1 \end{pmatrix} \boldsymbol{x}^{\downarrow} \le \begin{pmatrix} 1 & 1 & -1 & -1 \\ 2 & 0 & 0 & -2 \end{pmatrix} \boldsymbol{w} \right\}.$$

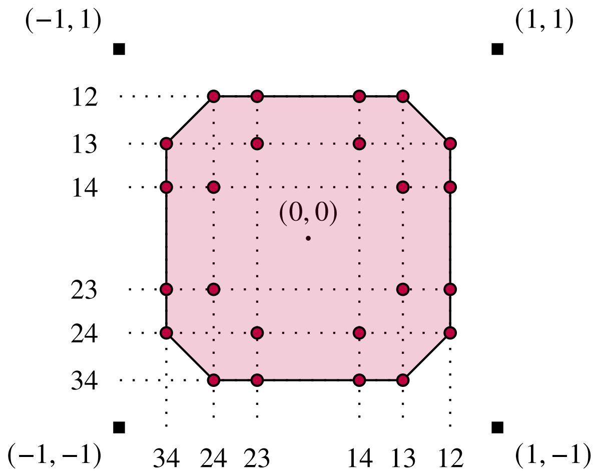

Figure 4. The 24 possible points are illustrated. The pair of numbers along the axis are shortcuts giving the indices of the w's that are positive, while the others are negative. For instance, the pair 14 represents the number $w_1 - w_2 - w_3 + w_4$.

Example 2.9 (Product of three segments, or the $[-1, 1]$-cube). Let us now consider the sweep polytope of $(\Delta_1)^3$, the product of three line segments. The case of general hypercubes is treated in detail later in Section 4. As in the previous example, we map $(\Delta_1)^3$ to $\mathbb{R}^3$ by taking the difference on each factor. The image is the cube $\square_3 = [-1, 1]^3 \subset \mathbb{R}^3$. This cube has 8 vertices, so if one computes the convex hull, $8! = 40320$ points need to be considered, of which only 96 form the convex hull; see Figure 5. Algorithms 3.4 and 3.6 determine directly these 96 vertices. The f-vector of this 8-lineup polytope is $(96, 144, 50)$; it has 24 square facets, 8 hexagonal facets, and 18 octagonal facets.

Using the $^{\downarrow}$-notation, we can write the H-representation as

$$\mathsf{L}(\square_3) = \left\{ \boldsymbol{x} \in \mathbb{R}^3 : \begin{pmatrix} 1 & 0 & 0 \\ 1 & 1 & 0 \\ 1 & 1 & 1 \\ 2 & 1 & 1 \end{pmatrix} \boldsymbol{x}^{\downarrow} \leq \begin{pmatrix} 1 & 1 & 1 & 1 & -1 & -1 & -1 & -1 \\ 2 & 2 & 0 & 0 & 0 & 0 & -2 & -2 \\ 3 & 1 & 1 & 1 & -1 & -1 & -1 & -3 \\ 4 & 2 & 2 & 0 & 0 & -2 & -2 & -4 \end{pmatrix} \boldsymbol{w} \right\}.$$

2.5. Certifying that a vector spans a ray

In general, a vector $\boldsymbol{y} \in \mathbb{R}^d$ may not induce a total order on $\mathbf{A}$ as there may be ties. Instead, the linear functional $\langle \boldsymbol{y}, \cdot \rangle$ induces an *ordered set partition*

$$\mathcal{S} = (S_1, \ldots, S_{k-1}, S_k)$$

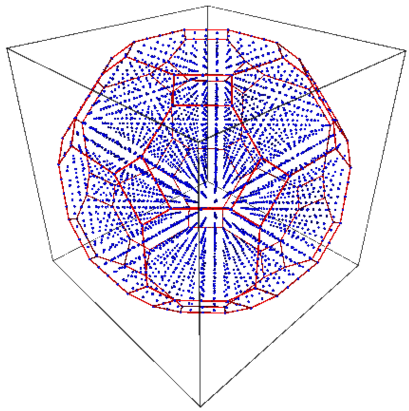

Figure 5. The convex hull of all 40320 occupation vectors arising from all permutations of the vertices of the cube $[-1, 1]^3$.

of $[n]$ as follows.

- For each $i = 1, \dots, k-1$, the set S_i consists of labels of points where the functional achieves the i-th largest value.
- We have $|S_1 \cup \cdots \cup S_{k-2}| < r$ and $|S_1 \cup \cdots \cup S_{k-1}| \geq r$.
- The last set S_k consists of everything else.

We call such an ordered set partition induced by some $\boldsymbol{y}$ an r-*ranking*. Faces of the r-lineup polytope $\mathsf{L}_r(\mathbf{A})$ are in bijection with r-rankings. We describe some linear programs that verify whether a given vector $\boldsymbol{y}$ induces an uncoarsenable r-ranking or not. For ease of notation, we focus on the case where r is maximal (and we drop the "r-" from the name), but the propositions below can be readily adapted to the general setup.

Proposition 2.10. *Let $\mathbf{A} = \{\boldsymbol{v}_1, \dots, \boldsymbol{v}_n\} \subset \mathbb{R}^d$, and let $\mathcal{S} = (S_1, S_2, \dots, S_k)$ be an ordered set partition of $[n]$. Fix $\{i_1, \dots, i_k\} \subset [n]$ with $i_j \in S_j$ for $j = 1, \dots, k$. For each integer $t \in [k-1]$, consider the linear program given by*

$$\begin{array}{lrcl} \textit{maximize} & \alpha_t, & & \\ \textit{subject to} & \langle \boldsymbol{y}, \boldsymbol{v}_a - \boldsymbol{v}_b \rangle & = & 0 \quad \textit{whenever } a, b \in S_k, \\ & \langle \boldsymbol{y}, \boldsymbol{v}_{i_{j+1}} - \boldsymbol{v}_{i_j} \rangle & = & \alpha_j \quad \textit{for } j = 1, \dots, k-1, \\ & (\boldsymbol{\alpha}, \boldsymbol{y}) & \in & \mathbb{R}^{k-1}_{\geq 0} \times \mathbb{R}^d. \end{array}$$

The ordered set partition $\mathcal{S}$ is a ranking if and only if the $k-1$ linear programs above each has a positive solution.

Proof. If $\mathcal{S}$ is a ranking, then there exists a vector $\boldsymbol{y} \in \mathbb{R}^d$ whose inner products on consecutive blocks strictly increase. This implies that there exist positive gaps $\alpha_1, \dots, \alpha_{k-1}$, proving the first direction.

Assume that the $k-1$ linear programs have non-zero solutions $(\alpha_1, \dots, \alpha_{k-1})$. As the origin satisfies the inequalities, the linear programs are feasible and the solutions satisfy $\alpha_i \geq 0$ for $i \in [k-1]$. A positive solution $\alpha_t > 0$ implies that the ranking induced by the corresponding $\boldsymbol{y}_t$ is a coarsening of $\mathcal{S}$ with S_t and S_{t+1} in different blocks. Therefore, the vector

$$\boldsymbol{y} = \sum_t \boldsymbol{y}_t$$

induces the common refinement of the induced ranking, which is equal to $\mathcal{S}$ by construction. ■

Since the face lattice of an r-lineup polytope is isomorphic to the poset of r-rankings ordered by coarsening, the facets correspond to the r-rankings that cannot be coarsened by any other r-ranking. We call such rankings geometrically *uncoarsenable*.

Proposition 2.11. *Let* $\mathbf{A} = \{\boldsymbol{v}_1, \dots, \boldsymbol{v}_n\} \subset \mathbb{R}^d$ *be a point configuration and*

$$\mathcal{S} = (S_1, S_2, \dots, S_k)$$

a ranking. Fix $\{i_1, \dots, i_k\} \subset [n]$ *with* $i_j \in S_j$ *for* $j = 1, \dots, k$. *For each integer* $t \in [k-1]$, *consider the linear program given by*

$$\begin{array}{lrcl} \textit{maximize} & \alpha_1 + \cdots + \alpha_{k-1}, & & \\ \textit{subject to} & \langle \boldsymbol{y}, \boldsymbol{v}_a - \boldsymbol{v}_b \rangle & = & 0 \quad \textit{whenever } a, b \in S_k, \\ & \langle \boldsymbol{y}, \boldsymbol{v}_{i_{j+1}} - \boldsymbol{v}_{i_j} \rangle & = & \alpha_j \quad \textit{for } j = 1, \dots, k-1, \\ & \alpha_t & = & 0, \\ & (\boldsymbol{\alpha}, \boldsymbol{y}) & \in & \mathbb{R}^{k-1}_{\geq 0} \times \mathbb{R}^d. \end{array}$$

The ranking $\mathcal{S}$ *is geometrically uncoarsenable if and only if zero is the solution to every* $k-1$ *linear program above.*

Proof. Assume that the t-th linear program has a positive solution. Then, there exists a vector $\boldsymbol{y}_t$ whose induced ranking is a coarsening of $\mathcal{S}$ such that (1) the points with indices in S_t and S_{t+1} are together in the same block, and (2) it has at least two blocks (since $\alpha_t > 0$). Therefore, $\mathcal{S}$ is geometrically coarsenable.

If $\mathcal{S}$ has a nontrivial coarsening $\mathcal{R}$ given by some vector $\boldsymbol{y}$, the coarsening must (1) contain at least two blocks and (2) merge two consecutive blocks of $\mathcal{S}$. Therefore, $\boldsymbol{y}$ provides a positive solution $\boldsymbol{\alpha}$ to a integer program for some $t \in [k-1]$. ■

As described in [28], combinatorial interpretations will be understood as #P problems. Here, we prove that, given a n point configuration $\mathbf{A}$ and an ordered set partition $\mathcal{S}$ of $[n]$, the problem of determining whether $\mathcal{S}$ corresponds to a facet of $\mathsf{L}_{r,\boldsymbol{w}}(\mathbf{A})$ is in NP.

Corollary 2.12. *The problem of counting the number of facets of the lineup polytope* $\mathsf{L}(\mathbf{A})$ *is in* #P.

Proof. Propositions 2.10 and 2.11 give a method to certify that an ordered set partition with k parts is realizable and uncoarsenable. This is done with $2k-2$ linear programs, each of which has n equalities, at most k inequalities and $d+k-1$ variables. Since each linear program can be solved in polynomial time [34, Theorem 13.4], the conclusion follows. ∎

3. General products of simplices

In this section, we study the lineup polytopes of product of simplices without any restrictions on their dimensions or their numbers. In the following section, we consider the case of products of segments. To ease the exposition, we treat the case where all simplices have the same dimension but everything extends to the general case.

3.1. Combinatorial algorithms

We first define an important poset that helps us navigate sweeps. For a standard reference on posets, see [36, Chapter 3].

Definition 3.1. Let $\boldsymbol{i}$ be the total order on the set $\{0,1,2,\dots,i\}$. Given integers d,N, let $P(d+1,N) := \boldsymbol{d}\times\cdots\times\boldsymbol{d}$ be the Cartesian product of N copies of $\boldsymbol{d}$. The *N-dimensional Young lattice* $J(P(d,N))$ consists of the lower-order ideals of $P(d,N)$.

By setting $N=2$ in Definition 3.1, we get that $J(P(d,N))$ is the usual Young lattice on Young diagrams contained in a $d\times d$ box, where boxes are indexed starting from 0 to $d-1$. This shift in indices is for practical purposes when $d=2$, having the indices 0 and 1 makes certain computations easier. Let Δ_{d-1} be the $(d-1)$-dimensional regular simplex whose vertices are the canonical basis vectors of $\mathbb{R}^d$. Define $\Pi_{d,N}\subset\mathbb{R}^{d\times N}$ as the Cartesian product $\Delta_{d-1}\times\cdots\times\Delta_{d-1}$ of N copies of Δ_{d-1}. The vertices of $\Pi_{d,N}$ are in natural bijection with the elements of the poset $P(d,N)$. Let $S=(s_1,\dots,s_N)\in P(d,N)$; we denote by

$$\boldsymbol{\chi}(S) = (\boldsymbol{e}_{s_1+1},\dots,\boldsymbol{e}_{s_N+1}) \in (\mathbb{R}^d)^N$$

the vertex of $\Pi_{d,N}$ associated with the element S. In order to obtain the lineup polytope of $\Pi_{d,N}$, we use symmetry.

Let $m > 0$ be a natural number. We denote by $\mathfrak{S}_m$ the group of bijections on the set $[m]$. The group $\mathfrak{S}_d \wr \mathfrak{S}_N$ acts naturally on $\mathbb{R}^{d\times N}$ and it fixes the polytope $\Pi_{d,N}$ and thus its normal fan. Thanks to these symmetries, we may, without loss of generality, recover all normal vectors by considering only the set of linear functionals in the *test cone* $\mathsf{T}_{d,N}$ in $\mathbb{R}^{d\times N}$, whose coordinates are all positive and increase in each factor. More precisely,

$$\mathsf{T}_{d,N} := \{\boldsymbol{x} \in \mathbb{R}^{d\times N} \mid 0 \le x_{1,j} \le \cdots \le x_{d,j} \text{ for } j \in [N]\}. \tag{3.1}$$

Due to the convention of ordering decreasingly the values to obtain a lineup, we momentarily need to consider *upper*-order ideals, for the following proposition to fit properly later. Upper order ideals in finite posets are in natural correspondence with *lower* order ideals.

Proposition 3.2. *Let $\ell = (\boldsymbol{v}_1, \ldots, \boldsymbol{v}_r)$ be an r-lineup of the vertices of $\Pi_{d,N}$ induced by a linear functional $\boldsymbol{y} \in \mathsf{T}_{d,N}$. The corresponding elements of the poset $P(d, N)$ form a upper-order ideal.*

Proof. For any $\boldsymbol{v} \in \Pi_{d,N}$, the defining linear inequalities of the test cone in equation (3.1) imply that all upper (in the poset) elements must have a larger value, hence coming earlier in the lineup. ■

Since any initial segment of a lineup is itself a lineup, then Proposition 3.2 gives us more refined information. An r-lineup of $\Pi_{d,N}$ is a *saturated chain of ideals of length r in the poset $J(P(d, N))$*. However, the opposite is not true; see [11, Section 9.3] for some examples that may be extended here and also [25, Introduction]. Nonetheless, we use this correspondence to generate all potential lineups for which we may recursively verify whether they are *realizable* or not using a set of inequalities in the test cone. The set of vectors $\boldsymbol{y}$ that yield a certain lineup turns out to be the set of certificates of feasibility of LPs that Mallows and Vanderbei used to obtain so-called *realizable* Young tableaux. Recursively constructing the certificates provides an efficient method to enumerate the realizable Young tableaux instead of performing an LP for each Young tableau; see Section 3.2.1. In [11], the potential lineups are refered to as *shifted ideals* and the *realizable* ones to the stricter notion of *threshold ideals*. To be correct, we should be referring to them as “saturated chains of length r exhausting a shifted or threshold ideal”, but that is rather wasteful.

We define $\mathscr{L}^r_{d,N}$ the normal fan of the lineup polytope $\mathsf{L}_{r,\boldsymbol{w}}(\Pi_{d,N})$, and as usual, we drop r from the notation when it is maximal. Instead of computing the complete normal fan, we compute its intersection with the test cone. This process induces a fan supported on the test cone that we call the *test fan* of $\mathsf{L}_{r,\boldsymbol{w}}(\Pi_{d,N})$ and denote it by $\mathcal{T}^r_{d,N}$. By restricting equation (2.5) to the test cone, we obtain the sequence

$$\mathsf{T}_{d,N} = \mathcal{T}^1_{d,N} \succeq \mathcal{T}^2_{d,N} \succeq \cdots \succeq \mathcal{T}_{d,N}.$$

When $r = 1$, $\mathcal{T}^1_{d,N}$ is simply the whole cone $\mathsf{T}_{d,N}$ and all of its faces.

Proposition 3.3. *Let τ be a ray of $\mathcal{T}^r_{d,N}$. The vector τ is a ray of $\mathcal{L}_{d,N}$, the fan of the sweep polytope $\mathsf{L}(\Pi_{d,N})$. However, τ is not necessarily a ray of $\mathcal{L}^r_{d,N}$.*

Proof. Since we are refining the fan at each step, it means that τ is a ray of $\mathcal{T}_{d,N}$. In the sweep polytope $\mathsf{L}(\Pi_{d,N})$, the interior of every lineup cone is either contained in the test cone $\mathsf{T}_{d,N}$ or disjoint from it. Indeed, a sweep induced by an element not in the test cone is necessarily different from one induced by a test element. This means that the normal fan of the sweep polytope intersected with the test cone, i.e., its test fan, is simply the set of the lineup cones contained in the test cone; there are no new cones generated by the intersection with $\mathsf{T}_{d,N}$. It follows that τ is a ray of $\mathcal{L}_{d,N}$, as sought. ∎

The algorithm described below is an adjusted version of [11, Algorithm F]. It yields all r-lineups of products of simplices. More precisely, we compute the lineup cones, as we need a certificate that an ordered list of r points is indeed a lineup. To obtain the lineup cones, we restrict the computation to their intersection with the test cone to consider each orbit exactly once and use recursion on r. The set of candidates to append to an r-lineup is taken from Proposition 3.2.

Algorithm 3.4 (Recursively construct lineups). *Let r, d, N be positive integers such that $1 \le r \le d^N$. The following procedure computes all r-lineups cones of the polytope $\Pi_{d,N}$ that intersect the interior of the test cone $\mathsf{T}_{d,N}$.*

Base case, $r = 1$. *If the vector $\boldsymbol{y}$ is in the test cone, then there is only one possibility: the normal cone of the vertex $\boldsymbol{e}_d \times \cdots \times \boldsymbol{e}_d$ intersected with the test cone is equal to the complete cone $\mathsf{T}_{d,N}$ whose H-representation is given in equation (3.1).*

Inductive step, $r > 1$. *Having all r-lineups together with their normal cones in $\mathsf{T}_{d,N}$, we proceed to obtain the $(r+1)$-lineups. For each r-lineup ℓ with cone K, the possible candidates for being in position $r+1$ are limited by the partial order on $J(P(d,N))$. Say there are candidates $C \subseteq J(P(d,N))$; then, $S \in C$ is allowed to be the next one if and only if the cone*

$$\mathsf{K} \cap \left\{ \boldsymbol{y} \in \prod_{j=1}^{N} \mathbb{R}^d : \langle \boldsymbol{y}, \boldsymbol{\chi}(S) \rangle \ge \langle \boldsymbol{y}, \boldsymbol{\chi}(S') \rangle, \text{ for all } S' \in C \setminus \{S\} \right\} \tag{3.2}$$

has the same dimension as that of K. *If so, then* (ℓ, S) *is an* $(r+1)$*-lineup and equation* (3.2) *describes its corresponding normal cone. Otherwise, we discard it.*

Given d and N as inputs, Algorithm 3.4 provides the V-representation of the sweep polytopes $\mathsf{L}(\Pi_{d,N})$ recursively through the parameter r. Equivalently, it computes the complete list of r-lineups together with certificates of their existence (actually the set of all certificates which is the lineup fan). The running time of Algorithm is output-polynomial (i.e., polynomial with respect to the size of the input and output) since the dimension of the polyhedron in equation (3.2) can be determined in polynomial time; see [34, Corollary 14.1g and the subsequent discussion]. The precise upper bound on the space used by Algorithm 3.4 is not known; below we give the obvious upper bound by bounding the size of C with respect to d and N. It would be interesting to determine a sharp upper bound on the size of C, given d, N, and r.

Question 3.5. What is the maximal number of facets of an r-lineup cone of the lineup fan of a product of N simplices of dimension $d-1$?

If we want to have the rays of the fan (i.e., to get the H-representation of the sweep polytope) and minimize the space used by the algorithm, it is better to make the H-representation in equation (3.2) irredundant. This can be done in polynomial time with respect to the number of inequalities and dimension; see, e.g., [13].

That being done, i.e., once Algorithm 3.4 is done, we may apply a $(H \to V)$-translation on each lineup cone and collect all (potential) generating rays of the lineup fan. This can be done in $O((|K| + |C|)d\ell)$ time, where $|K|$ is the number of irredundant inequalities used to represent K, $|C|$ is the number of candidates, and ℓ is the number of lineups found; see [4]. Finally, we may apply Algorithm 3.6, which certifies that a ray obtained by intersecting with the test cone is indeed a ray in the complete fan. As we use an LP to do so, having the V-representation of the sweep polytope along with the H-representations of the lineup cones as inputs, the verification below provides a polynomial running time algorithm to obtain the H-representation of the sweep polytope as output.

Algorithm 3.6 (Reduction step to obtain facets). *Algorithm 3.4 returns a list of cones with an H-representation given by equation* (3.2). *With this output, we can produce facet-defining inequalities for the lineup polytope by proceeding as follows. For each cone* K, *we do the following.*

(1) *Translate the cone into a V-representation to obtain its extremal rays.*

(2) *For each ray, we do the following.*

   (a) *Compute the induced ranking induced by it.*

   (b) *Use the linear program in Proposition 2.11 to check whether the ranking is uncoarsenable.*

(c) *If uncoarsenable, then the ray generates a facet-defining inequality. Else, discard; it is the product of intersecting a lineup cone with the test cone.*

Algorithms 3.4 and 3.6 together provide a double-representation algorithm that computes both representations simultaneously for the sweep polytopes $\mathsf{L}(\Pi_{d,N})$. There are two principal families of sweep polytopes $\mathsf{L}(\Pi_{d,N})$ that are of interest: those obtained by fixing d and letting $N \to \infty$ and fixing N and letting $d \to \infty$. The algorithm's strengths include the following.

(i) Recursiveness: when fixing N, this procedure can be used as a basis for a recursive algorithm to compute sequences of lineup polytopes as $d \to \infty$ by not recomputing a large part of the prefixes (not necessarily of hyperbox shape).

(ii) Trivial parallelization: lineups can be appended in parallel processes once candidates are enumerated.

(iii) Complexity: the complexity of the recursive step is obtained as follows. First, we generate the candidates. (This can be done in at most rd steps.) The upper bound on the number of candidates is the maximal size of an anti-chain of $P(d, N)$. This general problem was considered before (even by de Moivre in 1756 in some form); see, e.g., [8]. Therein, the authors provide exact asymptotical formulas extending previously studied ones. For fixed d, the number of candidates is bounded by $O(d^{N-1}/\sqrt{N})$ and for fixed N is it bounded by $g(N)d^{N-1} + O(d^{N-2})$, where $g(N)$ is a constant. The data in the article seem to indicate that $g(N)$ is between 0 and 1 and tends to 0 as $N \to \infty$. The authors provide the explicit bound for $N < 5$: for $N = 2$, there are at most d candidates, for $N = 3$, there are at most $3d^2/4$ (d even) and $(3d^2 + 1)/4$ (d odd), and for $N = 4$, there are $(2d^3 + d)/3$ candidates. The upper bound on the number of candidates limits the number of new inequalities to be added to the cone K and thus bounds the complexity of the LP used to determine the dimension of the intersection. Coincidentally, when fixing the dimension of all but a few simplices (which is the case for studying the product of two simplices), letting the dimension of the others tend to infinity does not affect the upper bound on the number of candidates (since the size of maximal anti-chains does not increase).

As an illustration, say that we are interested in fixing $N = 3$, and we are computing $d = 5$. The lineup polytope has dimension

$$N(d-1) = 12,$$

and the maximal number of new inequalities to append a lineup is at most

$$(3d^2 + 1)/4 = 19$$

(among 125 vertices). Therefore, as d increases, the ratio between the dimension of the lineup polytope and the maximal number of new inequalities will grow linearly,

	0	**3**	**8**	**11**
0	0	3	8	11
1	1	4	9	12
7	7	10	15	18

$\Rightarrow$

1	3	6	9
2	4	7	10
5	8	11	12

Figure 6. Values on the left and their relative positions on the right.

roughly by $d/4$. Thus, for a fixed number of simplices, Algorithms 3.4 and 3.6 provide (output)-polynomial time algorithms to obtain both representations.

(iv) Central symmetry: it plays a crucial role in the case of hypercubes. Indeed, due to central symmetry, lineups only need to be computed up to half the total length $r = 2^{N-1}$.

(v) Correct partial results: interrupting at any point Algorithm 3.4 leads to a list of cones whose rays may be certified to be facet defining inequalities of the lineup polytope.

Remark 3.7. If we are interested in rays of the sweep fan, then asserting rays in the last step by Proposition 3.3 is not necessary. Even though we may obtain non-facet-defining rays for the r-lineup fans with the previous steps, all the sweep cones are either contained test cone or have disjoint interior with the test cone, so any ray appearing there is an actual ray of the last fan, i.e., the sweep fan.

Question 3.8. Finally, we wonder whether it is possible to characterize the family of symmetric polytopes for which an adapted recursive procedure (for computing the lineup polytope), such as the one above, exists. As far as we know, this procedure works for hypersimplices, dilated simplices and products of them. Which other operations on polytopes could be done?

3.2. Examples

3.2.1. Product of two simplices. Using the test cone on the product of two simplices $\Delta_{e-1} \times \Delta_{f-1}$, we restrict ourselves to linear functionals of the form $(\boldsymbol{a}, \boldsymbol{b})$, where

$$0 = a_1 \leq a_2 \leq \cdots \leq a_e, \quad \text{and} \quad 0 = b_1 \leq b_2 \leq \cdots \leq b_f.$$

The values of the functional $(\boldsymbol{a}, \boldsymbol{b})$ on the vertices of $\Delta_{e-1} \times \Delta_{f-1}$ are the elements of the set $\{a_i + b_j : (i, j) \in [e] \times [f]\}$. We may arrange them in an $e \times f$ tableau and replace the entries by their relative order from 1 to $\boldsymbol{ab}$.

Example 3.9. For example, let $e = 3$, $f = 4$ and the linear functional $(\boldsymbol{a}, \boldsymbol{b}) = (0, 1, 7; 0, 3, 8, 11)$; then, the tableaux are given in Figure 6.

For any given vector $(\boldsymbol{a}, \boldsymbol{b})$, we consider the tableau of relative orders. A tableau T is a bijective function from $e \times f$ to $\{1, \ldots, e \times f\}$ that we usually depict as a filling of a rectangle as in Figure 6. By construction, this tableau is weakly increasing along rows and columns. Furthermore, it has the following properties:

$$\begin{aligned} &\text{if } T(i,j) = T(i,j+1) \quad \text{for some } i \in [e], \\ &\qquad\qquad \text{then } T(i,j) = T(i,j+1) \quad \text{for all } i \in [e], \end{aligned} \tag{3.3}$$

$$\begin{aligned} &\text{if } T(i,j) = T(i+1,j) \quad \text{for some } j \in [f], \\ &\qquad\qquad \text{then } T(i,j) = T(i+1,j) \quad \text{for all } i \in [f]. \end{aligned} \tag{3.4}$$

We call a tableau satisfying equations (3.3)–(3.4) a *constrained Young tableau*. If the vector is generic, there are no ties and the associated tableau of relative orders is a *standard Young tableau* or SYT for short. A tableau is called *realizable* if it is induced by a sweep; the definition originates from [25].

Example 3.10. When $e = 1$, the product is isomorphic to Δ_{f-1}. In this case, there is only one possible SYT and it is of course realizable. It follows that for simplex any ordering of its vertices is a sweep. Its sweep polytope is the permutohedron $\mathrm{Perm}(\boldsymbol{w})$. As long as $\boldsymbol{w}$ is strictly decreasing, the rays of its normal fan in the test cone are given by $(\underbrace{0, \ldots, 0}_{k}, \underbrace{1, \ldots, 1}_{f-k})$ for all $k \in [f-1]$.

The case $\boldsymbol{e} = 2$. In this case, every standard Young tableau is realizable, as was noted by Klyachko in [21, Example 4.1.2]. It also appears in [25, Section 2] and in [7, Theorem 7.10] in connection with monotone-path polytopes. We prove it once again to cover the case of rankings, not just sweeps.

Proposition 3.11. *Every constrained Young tableau of size $2 \times f$ is realizable.*

Proof. We can assume that $T(1,k) < T(2,k)$ for each k since if they are equal, then by equation (3.4) the first row is equal to the second and any constrained tableau of one row is realizable, so we can simply set $\boldsymbol{a} = (0,0)$ and use a $\boldsymbol{b}$ that realizes the first row.

We set $\boldsymbol{a} = (0,1)$ and we define $\boldsymbol{b}$ one step an the time. Start with $b_1 = 0$ so that initially we have $a_1 + b_1 = 0$ and $a_2 + b_1 = 1$. Assuming that $b_1, \ldots, b_k$ has been chosen so that the induced order is given by the relative order of first k columns of the tableau, we now choose b_{k+1}. Let ε be small enough and $k \geq 1$.

- If $T(1,k+1) = T(1,k)$, then by equation (3.3) we have $T(2,k+1) = T(2,k)$ and we set
$$b_{k+1} = 1 + b_k.$$
- Else, if $T(1,k+1) = T(2,j)$ for some $j \leq k$, then we set $b_{k+1} = 1 + b_j$.

- Else, $T(1,k+1)$ does not appear in the first k columns. If $T(1,k+1) < T(2,1)$, then we set $b_{k+1} = b_k + \varepsilon$. In this step, we need that $0 + b_k + \varepsilon = a_1 + b_{k+1} < a_2 + b_1 = 1 + 0 = 1$, which can be accomplished if ε is small enough. Otherwise, let j be the largest index such that $T(2,j) < T(1,k+1)$. We set $b_{k+1} = \max\{a_2 + b_j, a_1 + b_k\} + 1 + \varepsilon$. This ensures that

$$a_1 + b_{k+1} > \max\{a_2 + b_j, a_1 + b_k\}$$

but also that $a_1 + b_{k+1} < a_2 + b_j$ since $\varepsilon > 0$. ∎

It follows that the number of sweeps is equal to the number of SYT of shape $(2, f)$, which is equal to C_f, the f-th Catalan number.

Corollary 3.12. *The sweep polytope* $\mathsf{L}(\Delta_1 \times \Delta_{f-1})$ *has* C_f *orbits of vertices.*

Furthermore, we can also describe the set of facets. The following proposition is mentioned without proof in [21, Example 4.2.1].

Proposition 3.13. *The rays of the normal fan of* $\mathsf{L}(\Delta_1 \times \Delta_{f-1})$ *inside the test cone are*

$$\big(0,0;\underbrace{0,\dots,0}_{k},\underbrace{1,\dots,1}_{f-k}\big) \quad \textit{for all } k \in [f-1],$$

$$\big(0,1;\underbrace{0,\dots,0}_{p_1},\underbrace{1,\dots,1}_{p_2},\dots,\underbrace{k-1,\dots,k-1}_{p_k}\big) \quad \textit{for all partitions } p \vdash f.$$

Proof. We can assume that $a_2 > a_1 = 0$; otherwise, we are in the situation with one row and the first set of vectors arises from Example 3.10.

The rays in the test cone correspond to the uncoarsenable rankings which we now describe. Let T be the induced tableau associated to a ray $\boldsymbol{y}$. As mentioned above, we can assume that its rows are distinct. Even more, we can assume that it does not have two equal columns, as this case can be reduced to one with a smaller $f-1$. So, each entry appears at most twice in T.

Suppose that the number j appears only once and in the first row. Consider the ray obtained by merging the parts j and $j-1$ of $\boldsymbol{y}$; its induced tableau coarsens T. It follows that in an uncoarsenable ranking represented by T every element of the first row, except for 1 appears also in the second row and this implies that T is equal to

$$S(n) := \begin{array}{|c|c|c|c|c|}\hline 1 & 2 & 3 & \cdots & n \\ \hline 2 & 3 & 4 & \cdots & n+1 \\ \hline \end{array}.$$

In conclusion, every uncoarsenable tableau with different rows is equal to $S(n)$ or to a tableau obtained from $S(n)$ by duplicating columns. ∎

Example 3.14. By Proposition 3.13, we get that there are $f + p(f + 1)$ uncoarsenable tableau of size $2 \times f$, where $p(n)$ is the number of partitions of n. The list of uncoarsenable tableaux of size 2×3 is

1	2	3
2	3	4

,

1	1	2
2	2	3

,

1	2	2
2	3	3

,

1	1	2
1	1	2

,

1	2	2
1	2	2

.

The case $e \geq 3$. The situation is more complicated as not every tableau is realizable. Of all the 42 standard Young tableaux of size 3×3, exactly six are not realizable. For example, the tableau

1	2	6
3	5	7
4	8	9

is not realizable.

Here, we have the situation for $e = 3$ and different values of f.

Number of columns f	1	2	3	4	5	6	7	8
Realizable SYT	1	5	36	295	2583	23580	221680	2130493
Total SYT	1	5	42	462	6006	87516	1385670	23371634

As proved in [2, Corollary 1.4], the ratio between realizable tableaux and all tableaux tends to 0 as the number of column increases. In the following table, we record the total number of realizable standard tableaux of size $e \times f$ that we computed using Algorithm 3.4 implemented in SageMath. The bold entries are new contributions to the OEIS sequence [26, A211400].

e \\ f	1	2	3	4	5	6	7	8	9	10
1	1	1	1	1	1	1	1	1	1	1
2		2	5	14	42	132	429	1430	4862	16796
3			36	295	2 583	23 580	221 680	**2 130 493**	**20 829 605**	**206 452 585**
4				6 660	**152 933**	**3 533 808**	**81 937 118**			
5					**8 499 376**	**449 879 088**				

For $e = 2$, we have the Catalan numbers which grow as $O(4^f / f^{3/2})$. For $e = 3$, the least-square log-fit provides a rate of growth of ≈ 9.2808. For $e = 4$, the least-square log-fit provides a rate of growth of ≈ 23.0874. For $(3, 10)$, the computations took ≈ 93 cpudays. For $(4, 7)$, the computations took ≈ 31 cpudays. For $(5, 6)$, the computations took ≈ 199 cpudays. These computations used a basic parallel map-reduce procedure in SageMath to only count the number of lineups. An independent and optimized `C` implementation of the above algorithm for this specific problem on tableaux was used to verify the entries of the tableau and is available on GitHub [32].

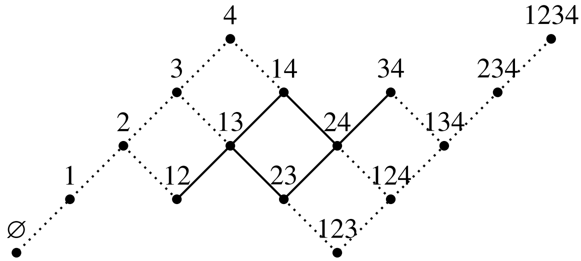

Figure 7. Extended Gale G(N) for $N = 4$ and the Gale poset on 2-subsets are illustrated with filled edges. In this figure, we depict the order from left to right as opposed to the usual bottom to top.

3.2.2. Product of three simplices. We computed the number of lineups for the following cases:

Number of vertices	Number of lineup orbits
$2 \times 2 \times 2$	12
$2 \times 2 \times 3$	110
$2 \times 3 \times 3$	3 792
$3 \times 3 \times 3$	566 616
$3 \times 3 \times 4$	80 638 740

The first cases are that of Example 2.9.

4. The case $d - 1 = 1$: Hypercubes

In the case of the products of line segments—that is of hypercubes—the associated group of symmetries is $\mathfrak{S}_2 \wr \mathfrak{S}_N$ which enjoys further properties. This is the *hyperoctahedral group* or Coxeter group of type B. We can refine the test cone and the Gale order previously defined.

Definition 4.1. The *(extended) Gale order* G(N) is the refinement of the Boolean lattice $2^{[N]} = \mathbf{1} \times \cdots \times \mathbf{1}$ given by the following relation. Recall that an element $S \in \mathbf{1} \times \cdots \times \mathbf{1}$ corresponds to a subset $S \subseteq [N]$. Given two subsets

$$S = \{s_1, \ldots, s_i\} \quad \text{and} \quad T = \{t_1, \ldots, t_j\},$$

with elements ordered from smallest to largest, we say that $S \leq T$ if and only if $|S| \leq |T|$ and $s_{i-k} \leq t_{j-k}$ for all $k \in \{0, \ldots, i-1\}$; see Figure 7 for an illustration with $n = 4$.

Remark 4.2. The poset $\mathrm{G}(N)$ is the poset $M(n)$ of minimal coset representatives of the subgroup of usual permutations $\mathfrak{S}_n$ within the Coxeter group of signed permutations B_n; see [35, Figure 6]. When this order is restricted to subsets of a fixed cardinality k, one recovers the traditional Gale poset on k-subsets of $[n]$; see Figure 7 for an example with $n = 4$ and $k = 2$.

We also define a refinement of the test cone (see equation (3.1)) by ordering the gaps between the vectors on each factor:

$$\mathsf{F}_{N,2} := \big\{\boldsymbol{x} \in \mathbb{R}^{2\times N} \mid 0 \leq x_{1,j} \leq x_{2,j} \text{ for } j \in [N] \\ \text{and } (x_{2,i} - x_{1,i}) \leq (x_{2,k} - x_{1,k}) \text{ whenever } i > k\big\}.$$

Furthermore, following Examples 2.8 and 2.9, we lower the dimension of the ambient space by considering the differences

$$\gamma : \mathbb{R}^{2\times N} \to \mathbb{R}^N, \quad (x_{1,j}, x_{2,j})_{j\in N} \mapsto (x_{2,j} - x_{1,j})_{j\in N}.$$

The map γ induces a linear isomorphism between the product of simplices $\Delta_1^N \subset \mathbb{R}^{2\times N}$ and the cube $[-1, 1]^N \subset \mathbb{R}^N$. The image, under γ, of the refined test cone $\mathsf{F}_{N,2}$ is the *fundamental chamber*:

$$\Phi_N = \{\boldsymbol{x} \in \mathbb{R}^N : x_1 \leq x_2 \leq \cdots \leq x_N\}.$$

Example 4.3. Let $n = 4$ and consider the sweep polytope of

$$\square_4 = [-1, 1]^4.$$

As opposed to the case $n = 3$ shown in Example 2.9, in this case brute force leads us nowhere, so we must rely on Algorithms 3.4 and 3.6. In this case, we obtain the following facet inequalities:

$$\mathsf{L}(\square_4) = \left\{ \boldsymbol{x} \in \mathbb{R}^4 : \begin{pmatrix} 1&0&0&0\\ 1&1&0&0\\ 1&1&1&0\\ 1&1&1&1\\ 2&1&1&0\\ 2&1&1&1\\ 2&2&1&1\\ 3&1&1&1\\ 3&2&1&1\\ 3&2&2&1\\ 4&2&1&1\\ 4&3&2&1 \end{pmatrix} \boldsymbol{x}^{\downarrow} \leq \begin{pmatrix} 1&1&1&1&1&1&1&1&-1&-1&-1&-1&-1&-1&-1&-1\\ 2&2&2&2&0&0&0&0&0&0&0&0&-2&-2&-2&-2\\ 3&3&1&1&1&1&1&1&-1&-1&-1&-1&-1&-1&-3&-3\\ 4&2&2&2&2&0&0&0&0&0&0&-2&-2&-2&-2&-4\\ 4&4&2&2&2&2&0&0&0&0&-2&-2&-2&-2&-4&-4\\ 5&3&3&3&1&1&1&1&-1&-1&-1&-1&-3&-3&-3&-5\\ 6&4&4&2&2&2&0&0&0&0&-2&-2&-2&-4&-4&-6\\ 6&4&4&4&2&2&2&0&0&-2&-2&-2&-4&-4&-4&-6\\ 7&5&5&3&3&1&1&1&-1&-1&-1&-3&-3&-5&-5&-7\\ 8&6&4&4&2&2&2&0&0&-2&-2&-2&-4&-4&-6&-8\\ 8&6&6&4&4&2&2&0&0&-2&-2&-4&-4&-6&-6&-8\\ 10&8&6&4&4&2&2&0&0&-2&-2&-4&-4&-6&-8&-10 \end{pmatrix} \boldsymbol{w} \right\}.$$

The length of a sweep of the set $[-1, 1]^N$ is 2^N and the number of sweeps, even when restricted to sweeps induced by functionals in the fundamental chamber, grows too fast for practical purposes. However, Remark 2.4 shows that we can obtain some of the inequalities for the sweep polytope by considering r-lineup polytopes. Indeed, setting $r = 2$, we get the inequalities in row 1 and 4, and incrementing r by 1, we sequentially get inequalities in rows 3 ($r = 3$), 7 ($r = 4$), 2 and 6 ($r = 5$), 9 ($r = 6$), 5 ($r = 7$), and finally 8, 10, 11, and 12 for $r = 8$.

Remark 4.4. In [11], we studied the case of indistinguishable fermionic particles: mathematically we considered a single Hilbert space $\mathcal{H}$ of dimension d and took its N antisymmetric power $\bigwedge^N \mathcal{H}$. Combinatorially, this led us to studying the sweep polytope of the *hypersimplex* $\Delta(d, N)$. For the case of N distinguishable qbits (so $d = 2$), the analogous polytope is the N-dimensional cube.

Whereas in [11], we considered d as a variable that was meant to grow to infinity, here for most applications a fixed d suffices. For practical purposes, what we need is to analyze what happens when N grows.

Proposition 4.5. *Let $r \geq 2$ and $N \geq r - 1$. Suppose that we have the H-representation*

$$\mathsf{L}_r([-1,1]^N) = \{\boldsymbol{x} \in \mathbb{R}^N : \langle \boldsymbol{y}, \boldsymbol{x}^{\downarrow} \rangle \leq b, (\boldsymbol{y}, b) \in I\},$$

where $I \subseteq \Phi_N \times \mathbb{R}$. For $M > N$, we have the H-representation

$$\mathsf{L}_r([-1,1]^M) = \{\boldsymbol{x} \in \mathbb{R}^M : \langle \boldsymbol{y}', \boldsymbol{x}^{\downarrow} \rangle \leq b', (\boldsymbol{y}, b) \in I\},$$

where $\boldsymbol{y}'$ is obtained from $\boldsymbol{y}$ by appending $M - N$ entries equal to y_1 at the beginning and $b' = b + (M - N)y_1$. With the exception that if $\boldsymbol{y} = (1, 0, \ldots, 0)$, then

$$\boldsymbol{y}' = (1, 0, 0, \ldots, 0).$$

Proof. The set of upper ideals of length r of the poset $\mathrm{G}(N)$ is isomorphic to that of $\mathrm{G}(M)$ as long as $N \geq r - 1$. The isomorphism is simply adding a 0 to every set and adding one to all elements (doing this $M - N$ times). When running Algorithm 3.4, we get the same steps and comparisons, with the only difference that the corresponding vectors have one more entry at the start, hence the replications of the first entry y_1. To obtain the new right-hand side b', we apply the last part of Proposition 2.3. ∎

For example, consider the following inequality for $N = 4$ which is minimal for $r = 4$:

$$(2, 2, 1, 1)\boldsymbol{x}^{\downarrow} \leq (6, 0, 0, -2)\boldsymbol{w},$$

where $\boldsymbol{w} = (w_1, w_2, w_3, w_4)$. It is transformed into the following inequality which is valid for $N = 7$ particles and $r = 4$:

$$(\mathbf{2}, \mathbf{2}, \mathbf{2}, 2, 2, 1, 1)\boldsymbol{x}^{\downarrow} \leq (6, 0, 0, -2)\boldsymbol{w} + 2(7 - 4).$$

Remark 4.6. The sweep polytope of $[-1,1]^n$ is normally equivalent to the sweep polytope of $[0,1]^n$. This is a zonotope obtained by Minkowski sum of the segments

$$\sum_{\boldsymbol{v}_1,\boldsymbol{v}_2\in\mathrm{Vert}([0,1]^n)} [\boldsymbol{0}, \boldsymbol{v}_1-\boldsymbol{v}_2].$$

The *resonance arrangement* is the hyperplane arrangement associated to the zonotope given by the Minkowski sum $\sum_{\boldsymbol{v}\in\mathrm{Vert}([0,1]^n)}(\boldsymbol{0},\boldsymbol{v})$. Dubbed the *White Whale* by Billera, some recent research have focused on the computations of its vertices; see [10, 15]. Since $\boldsymbol{0}$ is a vertex of $[0,1]^N$, the White Whale is a Minkowski summand of the sweep polytope of the cube. In other words, there exists a polytope Q such that

$$Q+\sum_{\boldsymbol{v}\in\mathrm{Vert}([0,1]^n)}[\boldsymbol{0},\boldsymbol{v}] = \sum_{\boldsymbol{v}_1,\boldsymbol{v}_2\in\mathrm{Vert}([0,1]^n)}[\boldsymbol{0},\boldsymbol{v}_1-\boldsymbol{v}_2]. \tag{4.1}$$

With a mix of clever ideas and lots of computational power, the total number of vertices of the White Whale is known only until $N=9$, see [15]. Equation (4.1) provides some context for the hardness of computing the sweep polytope of the cube.

5. Further questions

5.1. Relationship with the quantum marginal polytope

Even though the polytope $\Lambda(d,N,\boldsymbol{w})$ of equation (2.6) is not a sweep polytope, it contains some of the occupation vectors coming from lineups, namely, the ones in the positive orthant. We compare $\Lambda(d,N,\boldsymbol{w})$ and $\mathsf{L}_{r,\boldsymbol{w}}(\Pi_{d,N})$ in the following small example.

Example 5.1. Continuing Example 2.8, without loss of generality, we may restrict the study of $\mathsf{L}(\square_2)$ to the positive quadrant. In Example 2.8, we computed $\mathsf{L}(\square_2)$ the sweep polytope of the product of $N=2$ simplices of dimension $d-1$ with $d=2$. The inequalities obtained by Bravyi [9] for the polytope $\Lambda(2,2,\boldsymbol{w})$ are as follows:

$$\begin{aligned}
0\le x_1 \quad &\le w_1+w_2-w_3-w_4,\\
0\le \quad x_2 &\le w_1+w_2-w_3-w_4,\\
0\le x_1+x_2 &\le 2w_1-2w_4,\\
-2\min\{w_1-w_3,w_2-w_4\}\le x_1-x_2 &\le 2\min\{w_1-w_3,w_2-w_4\}.
\end{aligned}$$

The last two inequalities are the only ones that are not obtained by restricting $\mathsf{L}(\square_2)$ to the positive quadrant. The comparison between $\Sigma_{2,2,\boldsymbol{w}}$ restricted to the positive quadrant and $\Lambda(2,2,\boldsymbol{w})$ is illustrated in Figure 8, where

$$\mu := 2\min\{w_1-w_3,w_2-w_4\}.$$

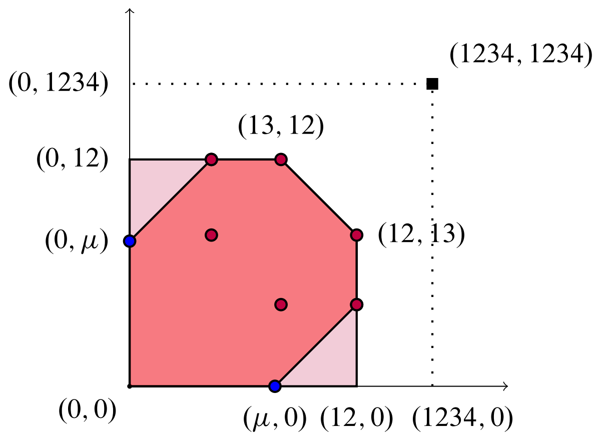

Figure 8. The 6 points illustrated from Figure 4 in the positive quadrant. We highlight that the two extra inequalities attain equality on some of these points.

In Figure 4, we assumed that $w_1 - w_2 - w_3 + w_4$ is larger than its negative $-w_1 + w_2 + w_3 - w_4$. This is equivalent to $w_1 - w_3 > w_2 - w_4$, in which case the maximum of $x_1 - x_2$ among the positive occupation vectors is

$$(w_1 + w_2 - w_3 - w_4) - (w_1 - w_2 - w_3 + w_4) = 2(w_2 - w_4).$$

Otherwise, if $w_1 - w_3 < w_2 - w_4$, then the positive occupation vectors include $(12, 23)$ and $(13, 23)$ instead of $(12, 14)$ and $(13, 14)$ in the terminology of Figure 4. In this case, the maximum value of $x_1 - x_2$ among the positive occupation vectors is $2(w_1 - w_3)$. In either case, the maximum value of $x_1 - x_2$ over the positive occupation vectors matches the maximum over the whole polygon $\Lambda(2, 2, \boldsymbol{w})$! Similarly, the same holds for the minimum.

Question 5.2. Does every facet defining inequality of the polytope $\Lambda(d, N, \boldsymbol{w})$ achieve its maximum over positive occupation vectors of the product of N simplices Δ_{d-1}? This would provide a closer relationship between $\mathsf{L}(\Delta_{d-1}^N)$ and $\Lambda(d, N, \boldsymbol{w})$.

5.2. Combinatorial interpretations of the H-representation of sweep polytopes of hypercubes

The H-representation given in Example 4.3 provides some material to investigate the following question.

Question 5.3. Is there a combinatorial interpretation for the right-hand side (and left-hand side) of the inequalities obtained in Example 4.3 that could deliver sufficient conditions for an inequality to be facet defining for sweep polytopes of higher-dimensional hypercubes?

5.3. Cyclic polytopes

Let $S = \{a_1, \dots, a_n\} \subset \mathbb{R}$ be a fixed subset of real numbers. The cyclic polytope $\mathsf{C}_d(S)$ is the convex hull of the set $\mathbf{C}_n := \{(1, a_i, a_i^2, \dots, a_i^{d-1}) : i \in [n]\} \subset \mathbb{R}^d$. The vertices of the cyclic polytope are naturally labeled by the set S. Furthermore, its face lattice and oriented matroid depend only on $n = |S|$ and not on the set S. A lineup of length n, i.e., a sweep, of the cyclic polytope consists of a total order of S coming from a linear functional $\boldsymbol{p} = (p_0, \dots, p_{d-1}) \in \mathbb{R}^d$. The value of the dot product in a vertex of the cyclic polytope is

$$(p_0, p_1, p_2, \dots, p_{d-1}) \cdot (1, a_i, a_i^2, \dots, a_i^{d-1}) = p_0 + p_1 a_i + \dots + p_{d-1} a_i^{d-1}.$$

In other words, we consider the polynomial $p(X) = p_0 + p_1 X + \dots + p_{d-1} X^{d-1} \in \mathbb{R}[X]$ and order the elements of S according to the values $p(S)$. Since the vector $\boldsymbol{p}$ is chosen arbitrarily, finding all lineups of $\mathbf{C}_n$ is equivalent to finding all possible orderings of n points induced by a *polynomial* of degree at most $d - 1$.

Question 5.4. Characterize the possible number of sweeps of the d-dimensional cyclic polytope with n-vertices. Are there closed formulas when $n \gg d$ for the maximal and minimal numbers?

Acknowledgments. The authors thank Alex Black, Jesus De Loera, Julia Liebert, Arnau Padrol, and Christian Schilling for helpful conversations. In particular, they are thankful to Vic Reiner for pointing out the connection with the poset in Remark 4.2. Sebastián Sánchez implemented the algorithm for counting realizable tableau in C. They are grateful to the Simons Center for Geometry and Physics, where a part of the work was carried out, and to Christian Schilling's group at the Ludwig Maximilian Universität München for their hospitality and providing a fruitful research atmosphere. They would like to thank Calcul Québec and the Digital Research Alliance of Canada for making advanced computing facilities available on Beluga and Narval, where the calculations in this article were carried out. Finally, they are grateful to the three referees for their carefully reading and suggestions.

Funding. FC was partially supported by FONDECYT Grant 1221133. JPL acknowledges the support of the Natural Sciences and Engineering Research Council of Canada (NSERC) [no. 2024-04140]. Cette recherche a été financée par le Conseil de recherches en sciences naturelles et en génie du Canada (CRSNG) [no. 2024-04140].

References

[1] M. Altunbulak and A. Klyachko, The Pauli principle revisited. *Comm. Math. Phys.* **282** (2008), no. 2, 287–322 Zbl 1159.81031 MR 2421478

[2] I. Araujo, A. E. Black, A. Burcroff, Y. Gao, R. A. Krueger, and A. McDonough, Realizable standard Young tableaux. 2023, arXiv:2302.09194v1

[3] D. Avis and D. Bremner, How good are convex hull algorithms? In *Proceedings of the eleventh annual symposium on computational geometry*, pp. 20–28, 1995

[4] D. Avis and K. Fukuda, A pivoting algorithm for convex hulls and vertex enumeration of arrangements and polyhedra. In *Proceedings of the seventh annual symposium on computational geometry*, pp. 98–104, 1991

[5] D. Avis and C. Jordan, mplrs: A scalable parallel vertex/facet enumeration code. *Math. Program. Comput.* **10** (2018), no. 2, 267–302 Zbl 1400.90222 MR 3804048

[6] A. Berenstein and R. Sjamaar, Coadjoint orbits, moment polytopes, and the Hilbert–Mumford criterion. *J. Amer. Math. Soc.* **13** (2000), no. 2, 433–466 Zbl 0979.53092 MR 1750957

[7] A. E. Black and R. Sanyal, Underlying flag polymatroids. *Adv. Math.* **453** (2024), article no. 109835 Zbl 07915897 MR 4776323

[8] D. Bouyssou, T. Marchant, and M. Pirlot, The size of the maximum antichains in products of linear orders. *TOP* **29** (2021), no. 3, 648–659 Zbl 1470.91020 MR 4292236

[9] S. Bravyi, Requirements for compatibility between local and multipartite quantum states. *Quantum Inf. Comput.* **4** (2004), no. 1, 12–26 MR 2045769

[10] T. Brysiewicz, H. Eble, and L. Kühne, Computing characteristic polynomials of hyperplane arrangements with symmetries. *Discrete Comput. Geom.* **70** (2023), no. 4, 1356–1377 Zbl 07781565 MR 4670362

[11] F. Castillo, J.-P. Labbé, J. Liebert, A. Padrol, E. Philippe, and C. Schilling, An effective solution to convex 1-body N-representability. *Ann. Henri Poincaré* **24** (2023), no. 7, 2241–2321 Zbl 1530.81148 MR 4603181

[12] D. R. Chand and S. S. Kapur, An algorithm for convex polytopes. *J. Assoc. Comput. Mach.* **17** (1970), 78–86 Zbl 0199.50902 MR 0278177

[13] K. L. Clarkson, More output-sensitive geometric algorithms. In *Proceedings of the IEEE Symposium held in Santa Fe, NM, November 20–22, 1994*, edited by S. Goldwasser, pp. 695–702, IEEE, 1994

[14] K. L. Clarkson and P. W. Shor, Algorithms for diametral pairs and convex hulls that are optimal, randomized, and incremental. In *Proceedings of the Fourth Annual Symposium on Computational Geometry (Urbana, IL, 1988)*, pp. 12–17, ACM, New York, 1988 MR 1213459

[15] A. Deza, M. Hao, and L. Pournin, Sizing the white whale. 2022, arXiv:2205.13309v1, to appear in *Fields Inst. Commun.*

[16] K. Fukuda, Polyhedral computation. 2020, https://www.research-collection.ethz.ch/handle/20.500.11850/426218, visited on 29 October 2024

[17] J. E. Goodman, J. O'Rourke, and C. D. Tóth (eds.), *Handbook of discrete and computational geometry*. Discrete Math. Appl. (Boca Raton), CRC Press, Boca Raton, FL, 2018 Zbl 1375.52001 MR 3793131

[18] C. Greene, A. Nijenhuis, and H. S. Wilf, A probabilistic proof of a formula for the number of Young tableaux of a given shape. In *Young tableaux in combinatorics, invariant theory, and algebra*, pp. 17–22, Elsevier, 1982

[19] L. Khachiyan, E. Boros, K. Borys, K. Elbassioni, and V. Gurvich, Generating all vertices of a polyhedron is hard. *Discrete Comput. Geom.* **39** (2008), no. 1-3, 174–190 Zbl 1147.05040 MR 2383757

[20] F. Kirwan, Convexity properties of the moment mapping. III. *Invent. Math.* **77** (1984), no. 3, 547–552 Zbl 0561.58016 MR 0759257

[21] A. Klyachko, Quantum marginal problem and representations of the symmetric group. 2004, arXiv:quant-ph/0409113v1

[22] A. A. Klyachko, Quantum marginal problem and n-representability. *J. Phys. Conf. Ser.* **36** (2006), no. 1, article no. 72

[23] L. Kühne, The universality of the resonance arrangement and its Betti numbers. *Combinatorica* **43** (2023), no. 2, 277–298 Zbl 07745876 MR 4627310

[24] C. Mallows, Deconvolution by simulation. In *Complex datasets and inverse problems*, pp. 1–11, IMS Lecture Notes Monogr. Ser. 54, Institute of Mathematical Statistics, Beachwood, OH, 2007 MR 2459175

[25] C. Mallows and R. J. Vanderbei, Which Young tableaux can represent an outer sum? *J. Integer Seq.* **18** (2015), no. 9, article no. 15.9.1 Zbl 1327.05334 MR 3401114

[26] OEIS Foundation Inc., The on-line encyclopedia of integer sequences. 2023, published electronically at http://oeis.org, visited on 29 October 2024

[27] A. Padrol and E. Philippe, Sweeps, polytopes, oriented matroids, and allowable graphs of permutations. *Combinatorica* **44** (2024), no. 1, 63–123 Zbl 07829394 MR 4707565

[28] I. Pak, What is a combinatorial interpretation? 2024, to appear in *Proceedings of the Open Problems in Algebraic Combinatorics*

[29] A. Postnikov, Permutohedra, associahedra, and beyond. *Int. Math. Res. Not. IMRN* **2009** (2009), no. 6, 1026–1106 Zbl 1162.52007 MR 2487491

[30] N. Ressayre, Geometric invariant theory and the generalized eigenvalue problem. *Invent. Math.* **180** (2010), no. 2, 389–441 Zbl 1197.14051 MR 2609246

[31] G. Rote, Degenerate convex hulls in high dimensions without extra storage. In *Proceedings of the eighth annual symposium on computational geometry*, pp. 26–32, 1992

[32] S. Sánchez and F. Castillo, Project ipi-23-2211. 2023, https://github.com/sebastian-sanchez-s/IPI-23-2211, version 1.0., visited on 29 October 2024

[33] C. Schilling, The quantum marginal problem. In *Mathematical results in quantum mechanics*, pp. 165–176, World Scientific, Hackensack, NJ, 2015 Zbl 1339.81104 MR 3381146

[34] A. Schrijver, *Theory of linear and integer programming*. John Wiley & Sons, 1998 Zbl 0970.90052

[35] R. P. Stanley, Weyl groups, the hard Lefschetz theorem, and the Sperner property. *SIAM J. Algebraic Discrete Methods* **1** (1980), no. 2, 168–184 Zbl 0502.05004 MR 0578321

[36] R. P. Stanley, *Enumerative combinatorics. Volume 1*. 2nd edn., Cambridge Stud. Adv. Math. 49, Cambridge University Press, Cambridge, 2012 MR 2868112

[37] H. R. Tiwary, On the hardness of computing intersection, union and Minkowski sum of polytopes. *Discrete Comput. Geom.* **40** (2008), no. 3, 469–479 Zbl 1155.52008 MR 2443296

[38] M. Vergne and M. Walter, Inequalities for moment cones of finite-dimensional representations. *J. Symplectic Geom.* **15** (2017), no. 4, 1209–1250 Zbl 1390.53095 MR 3734613

[39] A. Walfisz, *Weylsche Exponentialsummen in der neueren Zahlentheorie*. Mathematische Forschungsberichte 16, VEB Deutscher Verlag der Wissenschaften, Berlin, 1963 Zbl 0146.06003 MR 0220685

Communicated by Adrian Tanasă

Received 9 June 2023; revised 13 September 2024.

Federico Castillo
Facultad de Matematicas, Pontificia Universidad Católica de Chile,
Avenida Vicuña Mackenna 4860, Santiago, Chile; efecastillo.math@gmail.com

Jean-Philippe Labbé
Département des Enseignements Généraux, École de Technologie Supérieure,
1111 rue Notre-Dame Ouest, Montréal, H3C 6M8; Laboratoire d'Algèbre,
de Combinatoire et d'informatique Mathématique, UQAM, Case postale 8888,
Succursale centre-ville, Montréal, H3C 3P8, Canada; jean-philippe.labbe@etsmtl.ca